

A Quantitative Method using Near Infrared Imaging Spectroscopy for Determination of Surface Composition of Tablet Dosage Forms: an Example of Spirolactone Tablets

Renato L. Carneiro[#] and Ronei J. Poppi^{*}

Institute of Chemistry, University of Campinas (UNICAMP), CP 6154, 13083-970 Campinas-SP, Brazil

Neste trabalho, a espectroscopia de imagens no infravermelho próximo (NIR) foi empregada no estudo da distribuição do princípio ativo (API) espirolactona e seus excipientes em comprimidos. As análises foram realizadas utilizando resolução espacial de 50 μm , analisando 16 mm^2 de cada comprimido padrão. Modelos de mínimos quadrados parciais por intervalo (iPLS) foram utilizados para quantificação dos excipientes e API em cada pixel afim de obter mapas de concentração para cada composto. Foram obtidos erros de quantificação entre 0,49 e 1,26% quando realizada a validação cruzada utilizando a média espectral de cada comprimido. Esses modelos de calibração foram utilizados para prever a concentração individual de cada componente em cada pixel. A concentração média de todos os pixels, para cada composto, produziu erros entre 0,05 e 1,06%. Estes resultados indicaram que os modelos estavam aptos a quantificar todos os compostos em cada pixel, individualmente. Esta aproximação necessita ser realizada uma vez que não é possível conhecer a composição real em cada pixel.

In this work, near infrared (NIR) imaging spectroscopy was employed in the study of the distribution of the active pharmaceutical ingredient (API) spironolactone and its excipients in tablets. Analyses were performed using 50 μm spatial resolution to analyze 16 mm^2 of each standard tablet. Interval partial least squares models were used for API and excipients quantification in every pixel in order to obtain concentration maps for each compound. It was obtained errors of quantification between 0.49 and 1.26% when performed the cross-validation using spectral average of each tablet. These calibration models were used to predict individual concentration of each compound in the tablet, in every pixel. The average concentration of all pixels, for each compound yield errors, was between 0.05 and 1.06%. These results indicate that the models were able to quantify all compounds in each pixel. This approach is necessary since it is not possible to know the real concentration of each compound in the pixels.

Keywords: image spectroscopy, near infrared, spironolactone, content uniformity

Introduction

Pharmaceutical products prior to their approval for market authorization are evaluated and tested according to their quality test specification. These tests are: physical tests (appearance, average mass, etc.), chemical tests (assay, purity, etc.) and pharmaceutical tests (dissolution, content uniformity). Assay and content uniformity (CU) tests are two major aspects of drug quality assessment. Assay value reflects the mean active content in a production batch. The content uniformity test shows the distribution of the active

content within the production batch.¹⁻³ Production process of medicine presented as tablets involves some unitary operations: mixture, granulation, drying and compression. These unit operations must ensure that each tablet is within specification for dissolution, content uniformity, etc. Powder homogenization process is essential to obtain the correct amount of active pharmaceutical ingredient (API) in each tablet in order to satisfy the condition of content uniformity. However, the distribution of the particle size and density of the crystals greatly influence the forces that cause movement between the particles. So, the homogenization process is a critical step in the manufacturing process of tablets.²⁻⁵ An inefficient homogenization can result in some tablets with API concentration above correct content, and other tablets with the API concentration below correct

*e-mail: ronei@iqm.unicamp.br

[#]Current address: Department of Chemistry, Federal University of São Carlos (UFSCar), Rodovia Washington Luiz, km 235, 13565-905 São Carlos-SP, Brazil

content. This could directly affect the pharmaceutical efficiency of this medicine.

Spirolactone is a synthetic steroidal diuretic to treat a series of diseases, such as edema, cirrhosis of liver, hypokalemia and hypertension, and is used as antiandrogen agent.^{6,7}

Imaging spectroscopy is the combination between classic spectrometric methods and microscopic analysis. This technique produces hyperspectral images, which are cubes of data containing a spectrum by pixel. Raman,⁸ mid infrared,⁹ fluorescence¹⁰ and mass spectrometry¹¹ are techniques that can be adapted to perform imaging analysis. Imaging spectroscopy applied to characterization of compounds and spatial localization using near infrared (NIR) chemical imaging were demonstrated in pharmaceutical applications, such as mapping compound distribution, to verify the homogeneity or to detect counterfeits.¹²⁻¹⁸

In a review of the literature, it is possible to find that the principal method used to develop calibration models using imaging NIR data is the single wavelength approach, in which the intensity of a single wavelength is related to the concentration of a specific compound.^{14,17,19-23} It is obvious that the wavelength must be selective for the compound to be quantified, turning this a risky strategy. The principal multivariate method used to analyze NIR imaging data is the principal component analysis (PCA), however, PCA cannot be directly used as a prediction method for concentration.^{14,15,24-31} Other multivariate method is the classical least squares regression (CLS).^{18,22,32} CLS only requires the pure compound spectrum of each constituent in the sample in order to find their concentration by multivariate regression, but it does not work well if there are high noise levels and a high number of compounds in the sample. In addition, all spectra of compounds in the sample need to be known. Multivariate curve resolution-alternating least squares (MCR-ALS) is a multivariate method that is often used to generate calibration models using NIR imaging spectroscopy.^{27,31,33-35} It works similarly to CLS, but by alternating least squares, MCR-ALS can recover the concentration and spectra of analytes of interest and estimate the spectra of possible interferences. Unlike CLS, there is no need to know the pure spectra of the analytes to use MCR-ALS. However, MCR-ALS presents the same limitations of CLS, i.e., it does not work well if there are high noise levels and a high number of compounds in the sample. Partial least squares (PLS) is a well known multivariate calibration method that can be applied for very complex matrices. However, the concentration of the analyte of interest needs to be known to build the calibration model. There are few works using PLS due to

this restriction since it is impossible to perform reference analyses in just one pixel, but only in the whole sample. One of the main uses of PLS is to perform discriminant analysis (PLS-DA) in order to identify pixels that do not belong to the sample (interferences or contaminants).^{32,36,37} For quantification, most of works present PLS models built using pure spectra and do not take into account possible spectral changes due to interactions of the compounds.^{14,15,19,26,38-41} PLS is employed in few works to quantify compounds by NIR imaging using a calibration set,^{18,42-44} and none of them presented interval PLS (iPLS) to calculate concentration maps (chemical images) in tablets.

In this work, NIR imaging technique and iPLS were applied to simultaneously quantify API and three excipients in spironolactone tablets in order to find the chemical images of the tablet surface. This is an important criterion to study the homogeneity of compound in a single tablet, which is related to the manufacturing process quality.

Experimental

Materials and methods

HB43-S Halogen Moisture Analyzer from Mettler-Toledo was used to perform moisture analyses. Conventional NIR analyses were made using a NIR-FT Nicolet Antaris II by Thermo Scientific. Hyperspectral images from tablets were obtained using a Spotlight 400N NIR imaging system from Perkin-Elmer.

Multiplicative scattering correction algorithm, iPLS models and all treatments were performed using Matlab 2009B (Mathworks, Natick, MA, U.S.A).

Interval partial least squares

Interval partial least squares is a multivariate calibration method that generates different calibration models from different intervals of spectra (or from combinations of some intervals). This procedure is used to find spectral ranges that produce lower prediction errors (verified by cross-validation). Spectral ranges that have non-linear or no information are eliminated from the data matrix.⁴⁵⁻⁴⁷

A hyperspectroscopy image can be visualized as a cube of data since there are a lot of absorbance/reflectance values for each pixel. Each pixel can be considered as an individual sample in this technique, but the spatial information is preserved. To performed iPLS analysis in this kind of data, spectroscopic images need be unfolded to rearrange them as a data matrix. After the unfolding process, rows will be the spectra related to the different pixels in the data matrix.^{12,48}

Figure 1 shows a graphic illustration of iPLS prediction performed on a hyperspectral image.

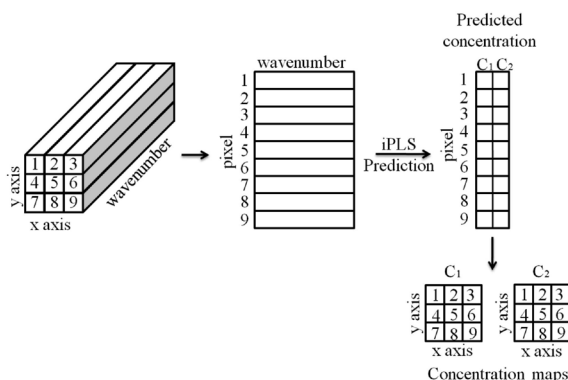


Figure 1. Graphic illustration of iPLS prediction. In this example, imaging analysis is performed on nine pixels. This cube of data is unfolded in a data matrix. Intervals prior selected are used to predict compound concentration in each pixel. Concentration matrix is refolded to produce concentration maps.

Standard tablet preparation

Tablets contained spironolactone (API), corn starch, calcium sulfate and polyvinylpyrrolidone (excipients). These excipients were selected based upon spironolactone commercial tablets. Concentrations of each excipient and API were around the concentration of commercial tablets to avoid compression problems such as capping, lamination, binding and others (proportions cannot be freely changed). These problems are solved by formulation work during commercial tablet development. Tablets were produced using a manual factoring process, in which excipients and API were mixed in plastic bags using previously defined proportions.

API and excipients raw material had some water content that was measured for each excipient and API using the moisture analyzer. Water was not considered an excipient in the tablet, but real content of each excipient was corrected before calibration and prediction procedure. Average water content for all standards was around 11%,

so water was not considered a variable in this experimental design.

Standard tablets were produced by using an experimental design based upon ideal concentration of excipients from commercial samples. So, it was prepared an ideal concentration mixture (IM) containing: spironolactone (SP), calcium sulfate (CA), corn starch (CS) and polyvinylpyrrolidone (PV). Standards were obtained by addition of SP, CA, CS and PV in this ideal mixture. As explained before, changes in excipient compositions cannot be freely made due to compression problems.

There were four substances to perform the experimental design: SP, CA, CS and PV. PV had lower concentration than other excipients in the commercial sample. So, it was performed a ternary mixture design using three major compounds presented in the tablet: SP, CA and CS. Ten standards were yielded performing this ternary design, providing five variation levels for each compound. It was added different concentrations of PV to each standard to quantify this compound. It were produced five tablets for each of the ten standards.

Standards were prepared using 300 mg of IM. To this amount, it was added 60 mg of different combinations of SP, CA and CS following a ternary design. Average weight of commercial tablet was around 360 mg, for this reason, total weight of standard tablets was 360 mg, before addition of PV. Ternary mixture design has a constraint: the sum of all compounds is 100% for all standards. Since 100% of variation in this design is 60 mg, the constraint will be: $SP + CA + CS = 60$ mg. This design is known as ternary mixture design using pseudocomponents since variation occurs on a previously fixed condition.⁴⁹

Standards were prepared according to Table 1. Bracket values show the real concentration (%) of each compound in each standard tablet. Real concentration was obtained by discounting the moisture percentage for each raw material. Moisture content in the standards was calculated by the percentage of water content in each raw material.

Table 1. Experimental design (mg) without moisture correction. Brackets show real percentage for each compound in the standards after moisture and weight corrections

Standard	Standard composition / mg (%)									
	1	2	3	4	5	6	7	8	9	10 (IM)
IM	300	300	300	300	300	300	300	300	300	360
SP	60 (27.74)	0 (12.12)	0 (12.28)	30 (20.66)	30 (20.95)	0 (12.45)	40 (23.08)	10 (14.78)	10 (14.59)	0 (15.14)
CA	0 (22.76)	60 (36.24)	0 (23.37)	30 (30.46)	0 (24.02)	30 (30.46)	10 (25.60)	40 (31.85)	10 (24.92)	0 (28.83)
CS	0 (31.72)	0 (32.14)	60 (46.95)	0 (33.02)	30 (40.87)	30 (40.31)	10 (34.97)	10 (34.51)	40 (41.05)	0 (40.18)
PV	20 (7.81)	15 (6.68)	10 (5.52)	5 (4.32)	0 (3.09)	5 (4.32)	10 (5.52)	15 (6.68)	20 (7.81)	0 (3.71)
Moisture	(9.97)	(12.82)	(11.89)	(11.53)	(11.07)	(12.46)	(10.83)	(12.19)	(11.63)	(12.14)

A hydraulic press was used to compress the mixture of powders yielding the tablets. It was used 2.5 tons *per* in² pressure. Standard tablets were circular (8 mm diameter) having plane surfaces.

Conventional NIR reflectance analysis

NIR-FT Nicolet Antaris II was used to obtain reflectance spectra from standard tablets. It was used 8 cm⁻¹ spectral resolution, 10000-4000 cm⁻¹ spectral range and 16 scans. By conventional analysis, it would be possible to detect experimental design errors and the quantitative prediction performance of this calibration set by cross-validation. Conventional NIR reflectance analysis uses larger spotlight to avoid heterogeneity problems. By using an iris, whole tablet surface could be radiated.

Imaging NIR reflectance analysis

Imaging analyses of yielded tablets were performed by reflectance technique using the Spotlight 400N NIR imaging system, 50 μm spatial resolution, 16 cm⁻¹ spectral resolution, 7800-3800 cm⁻¹ spectral range and 4 scans. It was analyzed a square with 16 mm² (4000 μm × 4000 μm) area in the center of the tablets for each standard, resulting in 50 hyperspectral images containing 80 × 80 pixels, i.e., 6400 spectra or pixels *per* image. Approximately 1 h was spent to acquire each hyperspectral image.

Results and Discussion

Preliminary results of conventional analysis by NIR reflectance spectroscopy

A multiplicative scattering correction (MSC) procedure was used to correct the spectra from conventional NIR reflectance analysis. Smoothing processes were performed by a moving average. For calculations, it was used first derivate spectra.

It was performed PCA analysis for each replicate set to find possible outliers (this analysis is necessary due to homogeneity problems since reflectance analysis is partially a surface analysis). Results show that all standards were correctly prepared since results obtained for each replicate set needed just a component to explain more than 99.36% of variance from treated data.

A PLS model was performed with treated data. Absolute errors obtained by cross-validation (leave-five-out, taking off all replicates of each standard from the calibration set) were: 1.38% to SP, 0.89% to CA, 1.21% to CS and 1.19% to

PV. Four latent variables were used in this cross-validation analysis for each compound.

Quantitative analysis using iPLS for imaging spectroscopy data

In solid preparations, a perfect homogenization is impossible. It is common to have particles whose dimensions are contained between 10-500 μm. This is not a problem in the product quality. By contrast, the particle size is a feature that should be tightly controlled to maintain the bioavailability of the API similar in different batches. Thus, it is expected to find points in which there is an agglomeration of excipients or API due to the presence of larger crystals of these substances. The pixel size in this application was 50 μm × 50 μm and then, 200 micron particles can be viewed by four pixels in the hyperspectral images. Reflectance analysis is a surface analysis, but NIR radiation can penetrate inside the sample. Penetration power of NIR radiation is sample composition and wavelength dependent, reaching up micrometers to millimeters, for lower absorptive wavelengths. This feature implies that, although there are crystals of a pure substance on the tablet surface, NIR radiation can pass through the crystal on surface and still pass for crystals of other substances inside of tablet. It is hard to find pixels containing a pure substance signal due to high penetration power of NIR radiation.

Concentration maps were found for all tablets, but in this work, it will be presented only the results for the first replicate of eighth standard since it presents highest heterogeneity.

Tablet spectra and real concentrations of substances of interest are required to build a PLS (or iPLS) calibration model. It is impossible to obtain the real concentration of compounds in each pixel, but total concentration in the whole tablet is known. To overcome this problem, an average spectrum from all pixels of each tablet was used to build the calibration models.

Cross-validation errors were used to examine the validity of the models using average spectra of tablets. In order to minimize calibration errors, it was performed PLS models using some intervals of spectra (iPLS procedure). NIR spectra were split in five parts and calibration models were developed for each analyte using each part of the spectra. Table 2 shows the average errors of the best models to each compound, as well as the range of the spectrum used for calibration and the number of PCs.

As presented in Table 2, SP, CA and CS have the same optimal range to build the calibration models. This occurs because NIR spectroscopy is a non-selective method based on molecular overtone and combination vibrations, i.e.,

same wavenumbers can bring information from distinct compounds and/or chemical bonds.

Table 2. Description of best models for each compound: spectral ranges, number of PCs and absolute error. Models created using average spectra of tablets and evaluated by cross-validation leave-five-out (all replicate set)

	SP	CA	CS	PV
Interval / cm^{-1}	4696-3920	4696-3920	4696-3920	6248-5472
Number of PCs	4	3	3	3
Average absolute error / %	0.70	0.94	1.26	0.49

After building calibration models with the spectra average from all pixels for each tablet, these models were used to predict the analytes using spectra from each pixel. Spatial information was maintained even after unfolding operation, so concentration maps were constructed using predicted concentration for each analyte in each pixel. Four concentration maps were obtained for each tablet. These maps show the distribution of each component on the tablet surface. Figure 2 presents concentration maps for SP, CA, CS and PV for the first replicate of eighth standard. In addition, it was calculated the total concentration map, which provides the sum of the percentage of four monitored substances in each pixel. Expected total percentage for the sum of concentrations for the four substances is around 89%, as previous explained, since moisture in tablets was around 11% (Table 1).

Concentration maps indicate that when there is an accumulation of some substances at certain points of the tablet, there will be a deficit in the concentration of other substances in those pixels. This feature can be especially seen for calcium sulfate and polyvinylpyrrolidone in Figure 2, where there are high accumulation of calcium sulfate and polyvinylpyrrolidone at some points probably due to large crystals of these substances. Table 3 presents the concentration values obtained for the tablet (eighth standard) as a whole, using the average concentration in pixels found by iPLS model. It also presents the errors and standard deviation of concentration between pixels, for each compound.

Total concentration map in Figure 2 shows a homogeneous distribution profile confirming the good prediction of the model since total concentration sum of all analytes will always be around the expected, approximately 89% in each pixel. Lower standard deviation values of predicted concentrations in the pixels indicate higher homogeneity of analytes in the tablets. Higher standard deviation implies lower homogeneity since predicted concentration will be so different between pixels due to heterogeneity. As presented in Figure 2, it was expected higher values of standard deviation to CA and PV due to higher heterogeneity in these concentration maps.

The standard deviation of the concentration among the pixels do not depends if the substance is in a cluster or not, i.e., it does not depends of the spatial distribution. Indeed, the standard deviation will be affected by the fraction of

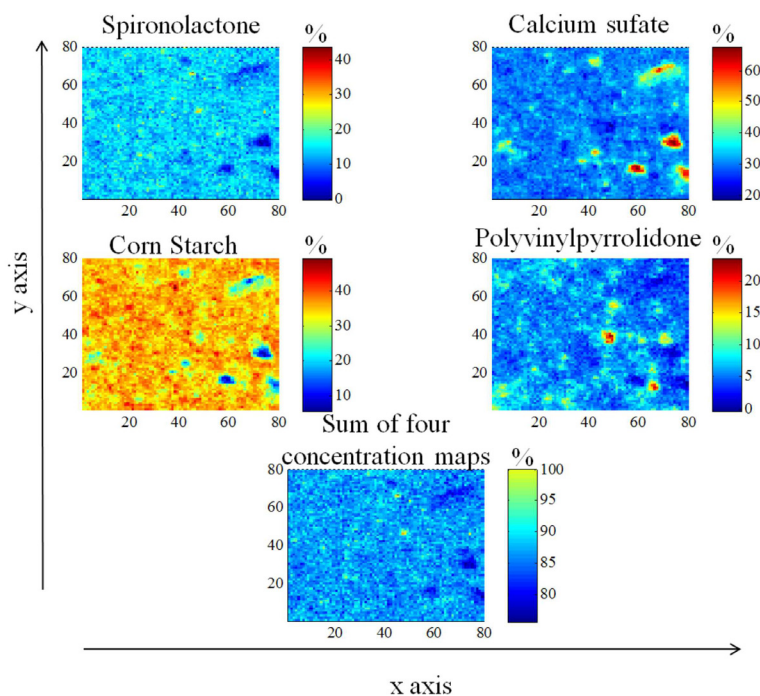


Figure 2. Concentration maps of first replicate from eighth standard. Vertical bars indicate percentage values related to total composition.

Table 3. Predicted values for four analytes using the average predicted concentration of pixels and standard deviation of the concentration (as percentage of the real value) among pixels for each compound (eighth standard)

Analite	Predict / %	Real / %	Error / %	Pixel standard deviation / %
Spirolactone	13.72	14.78	-1.06	19.24
Calcium sulfate	31.80	31.85	-0.05	14.44
Corn starch	34.97	34.51	0.46	11.30
Polyvinylpyrrolidone	6.09	6.68	0.59	35.14
Total ^a	86.58	87.82	-1.24	2.82

^aSum of percentage of analytes in every pixels.

pixels that contain some amount of the analyte. PV had the highest standard deviation due to its low concentration in tablet composition. For SP, CA and CS, relative standard deviations were similar.

There is not a parameter that defines if a simple tablet is homogeneous according to any pharmacopoeia. This occurs due to the fact that a whole tablet must be administered, without breaking it in two or more pieces. Currently, the homogeneity is measured among tablets, in which the standard deviation of the concentration of the active ingredient should not be more than 6%, and the API average content must range from 95 to 105% for tablets which weigh more than 250 mg, according to the Brazilian Pharmacopoeia.⁵⁰

Conclusions

Preliminary analysis of the standards using conventional reflectance NIR spectroscopy showed that standards were correctly prepared and obtained acceptable prediction errors by cross-validation. Even using a small number of experiments and using average spectra of tablets to develop the calibration models, absolute errors of the models using spectroscopic images were acceptable (between 0.49 and 1.26%) when performed iPLS models with cross-validation.

iPLS quantitatively confirmed the presence of each compound in each pixel. Total concentration map shows that the prediction of concentration in the pixels was correctly performed as the sum of the percentages of all components is around 88%. This is the expected one since there was 12.19% of water in the analyzed tablet - the eighth standard.

Prediction of the absolute errors found using average predicted concentration in the pixels are according to the expected values (between -0.05 and 1.06%) found by previous analysis using conventional NIR spectroscopy, confirming the consistency of the models.

This work demonstrated that NIR imaging is a powerful analytical tool in the study of tablets. If NIR imaging is used instead of conventional NIR spectroscopy, the detection limit of an API at low concentration could decrease since

a single crystal in a tablet could be responsible for the total signal in a single pixel (50 μm). In addition, NIR imaging can be used to evaluate the efficiency of the process of homogenization of the excipients and API in the tablets manufacturing process.

References

1. Bánfai, B.; Ganzler, K.; Kemény, S.; *J. Chromatogr., A* **2007**, *1156*, 206.
2. *The European Pharmacopoeia*, 6th ed. (6.2); European Directorate for the Quality of Medicines & Healthcare: Strasbourg, 2008.
3. Peck, G. E.; Baley, G. J.; McCurdy, V. E.; Banker, G. S. In *Pharmaceutical Dosage Forms: Tablets*, vol. 1, 2th ed.; Lieberman, H. A.; Lachman, L.; Schwartz, J. B., eds.; Marcel Dekker Inc.: New York, 1989, ch. 2.
4. Huang, C. Y.; Ku, M. S.; *Int. J. Pharm.* **2010**, *383*, 70.
5. Johnson, K. C. In *Formulation and Analytical Development for Low-Dose Oral Drug Products*; Zheng, J. Y., ed.; John Wiley & Sons: New Jersey, 2009, ch. 3.
6. Dong, Y.; Ng, W. K.; Shen, S.; Kim, S.; Tan, R. B. H.; *Int. J. Pharm.* **2009**, *375*, 84.
7. Rathnayake, D.; Sinclair, R.; *Dermatol. Clin.* **2010**, *28*, 611.
8. Zhang, L.; Henson, M. J.; Sekulic, S. S.; *Anal. Chim. Acta* **2005**, *545*, 262.
9. Van Eerdenbrugh, B.; Taylor, L. S.; *Int. J. Pharm.* **2011**, *417*, 3.
10. Leblond, F.; Davis, S. C.; Valdés, P. A.; Pogue, B. W.; *J. Photochem. Photobiol., B* **2010**, *98*, 77.
11. van Hove, E. R. A.; Smith, D. F.; Heeren, R. M.; *J. Chromatogr., A* **2010**, *1217*, 3946.
12. Amigo, J. M.; Ravn, C.; *Eur. J. Pharm. Sci.* **2009**, *37*, 76.
13. Lewis, E. N.; Carroll, J. E.; Clarke, F.; *NIR News* **2001**, *12*, 16.
14. Lewis, E. N.; Schoppelrei, J.; Lee, E.; Kidder, L. H. In *Process Analytical Technology*, Bakeev, K. A., ed.; Blackwell Publishing Ltd: Oxford, 2005, ch. 7.
15. Clarke, F.; *Vib. Spectrosc.* **2004**, *34*, 25.
16. Roggo, Y.; Edmond, A.; Chalus, P.; Ulmschneider, M.; *Anal. Chim. Acta* **2005**, *535*, 79.

17. Roggo, Y.; Jent, N.; Edmond, A.; Chalus, P.; Ulmschneider, M.; *Eur. J. Pharm. Biopharm.* **2005**, *61*, 100.
18. Gendrin, C.; Roggo, Y.; Collet, C.; *Talanta* **2007**, *73*, 733.
19. Lyon, R. C.; Lester, D. S.; Lewis, E. N.; Lee, E.; Yu, L. X.; Jefferson, E. H.; Hussain, A. S.; *AAPS PharmSciTech.* **2002**, *3*, 1.
20. El-Hagrasy, A. S.; Morris, H. R.; D'Amico, F.; Lodder, R. A.; Drennen III; J. K.; *J. Pharm. Sci.* **2001**, *90*, 1298.
21. Jovanovic, N.; Gerich, A.; Bouchard, A.; Jiskoot, W.; *Pharm. Res.* **2006**, *23*, 2002.
22. Gendrin, C.; Roggo, Y.; Spiegel, C.; Collet, C.; *Eur. J. Pharm. Biopharm.* **2008**, *68*, 828.
23. Sasic, S.; *Appl. Spectrosc.* **2007**, *61*, 239.
24. Burger, J.; Geladi, P.; *J. Near Infrared Spectrosc.* **2007**, *15*, 29.
25. Hilden, L. R.; Pommier, C. J.; Badawy, S. I. F.; Friedman, E. M.; *Int. J. Pharm.* **2008**, *353*, 283.
26. Ma, H.; Anderson, C. A.; *J. Pharm. Sci.* **2008**, *97*, 3305.
27. Amigo, J. M.; Cruz, J.; Bautista, M.; Maspoch, S.; Coello, J.; Blanco, M.; *TrAC, Trends Anal. Chem.* **2008**, *27*, 696.
28. Kamruzzaman, M.; El Masry, G.; Sun, D. W.; Allen, P.; *J. Food Eng.* **2011**, *104*, 332.
29. Puchert, T.; Lochmann, D.; Menezes, J. C.; Reich, G.; *J. Pharm. Biomed. Anal.* **2010**, *51*, 138.
30. Rahman, Z.; Zidan, A. S.; Khan, M. A.; *Eur. J. Pharm. Biopharm.* **2010**, *76*, 127.
31. Carneiro, R. L.; Poppi, R. J.; *J. Pharm. Biomed. Anal.* **2012**, *48*, 42.
32. Amigo, J. M.; Ravn, C.; Gallagher, N. B.; Bro, R.; *Int. J. Pharm.* **2009**, *373*, 179.
33. Franch-Lage, F.; Amigo, J. A.; Skibsted, E.; Maspoch, S.; Coello, J.; *Int. J. Pharm.* **2011**, *411*, 27.
34. Cruz, J.; Bautista, M.; Amigo, J. M.; Blanco, M.; *Talanta* **2009**, *80*, 473.
35. Cruz, J.; Blanco, M.; *J. Pharm. Biomed. Anal.* **2011**, *56*, 408.
36. van den Broek, W. H. A. M.; Derks, E. P. P. A.; van de Ven, E. W.; Wienke, D.; Geladi, P.; Buydens, L. M. C.; *Chemom. Intell. Lab. Syst.* **1996**, *35*, 187.
37. Nicolai, B. M.; Lötze, E.; Peirs, A.; Scheerlinck, N.; Theron, K. I.; *Postharvest Biol. Technol.* **2006**, *40*, 1.
38. Westenberger, B. J.; Ellison, C. D.; Fussner, A. S.; Jenney, S.; Kolinski, R. E.; Lipe, T. G.; Lyon, R. C.; Moore, T. W.; Revelle, L. K.; Smith, A. P.; Spencer, J. A.; Story, K. D.; Toler, D. Y.; Wokovich, A. M.; Buhse, L. F.; *Int. J. Pharm.* **2005**, *306*, 56.
39. Koehler, F. W.; Lee, E.; Kidder, L. H.; Lewis, E. N.; *Spectrosc. Eur.* **2002**, *14*, 12.
40. Furukawa, T.; Sato, H.; Shinzawa, H.; Noda, I.; Ochiai, S.; *Anal. Sci.* **2007**, *23*, 871.
41. Weiyong, L.; Woldu, A.; Kelly, R.; McCool, J.; Bruce, R.; Rasmussen, H.; Cunningham, J.; Winstead, D.; *Int. J. Pharm.* **2008**, *350*, 369.
42. ElMasry, G.; Sun, D. W.; Allen, P.; *Food Res. Int.* **2011**, *44*, 2624.
43. Ravn, C.; Skibsted, E.; Bro, R.; *J. Pharm. Biomed. Anal.* **2008**, *48*, 554.
44. Wold, J. P.; O'Farrell, M.; Høy, M.; Tschudi, J.; *Meat Sci.* **2011**, *89*, 317.
45. Borin, A.; Poppi, R. J.; *Vib. Spectrosc.* **2005**, *37*, 27.
46. Chen, Q.; Zhao, J.; Liu, M.; Cai, J.; Liu, J.; *J. Pharm. Biomed. Anal.* **2008**, *46*, 568.
47. Pereira, A. F. C.; Pontes, M. J. C.; Neto, F. F. G.; Santos, S. R. B.; Galvão, R. K. H.; Araújo, M. C. U.; *Food Res. Int.* **2008**, *41*, 341.
48. de Juan, A.; Tauler, R.; Dyson, R.; Marcolli, C.; Rault, M.; Mader, M.; *TrAC, Trends Anal. Chem.* **2004**, *23*, 70.
49. Bruns, R. E.; Scarmínio, I.; Neto, B. B.; *Statistical Design – Chemometrics*; Elsevier Science & Technology: Amsterdam, 2006.
50. *Farmacopeia Brasileira*, 5a. ed.; Agência Nacional de Vigilância Sanitária: Brasília, Brasil, 2010.

Submitted: February 7, 2011

Published online: August 9, 2012

FAPESP has sponsored the publication of this article.